



Article

Tribological and Micro-Mechanical Properties of Injected Polypropylene Modified by Electron Radiation

Martin Ovsik * Michal Stanek and Adam Dockal

Faculty of Technology, Tomas Bata University in Zlin, Vavreckova 5669, 760 01 Zlin, Czech Republic; stanek@utb.cz (M.S.); a_dockal@utb.cz (A.D.)

* Correspondence: ovsik@utb.cz

Abstract: Today, more and more importance is given to the improvement of polymer materials' wear resistance, i.e., their micro-mechanical and tribological properties, which could widen their application in practice. The properties of materials can be modified by several methods, among them exposure to electron radiation. This study focuses on the effect of varying radiation intensity (15 kGy to 99 kGy), depth of penetration, and subsequent structure modification of injection-molded polypropylene on tribological and micro-mechanical properties. Electron radiation influences the structure of individual layers, thus improving or degrading their properties. Hence, the depth of penetration can be examined by instrumented hardness tests and scratch tests. Due to irradiation, surface properties and wear resistance increased by up to 105% (from 38 MPa to 78 MPa). As the results show, an increase in mechanical properties was recorded in the direction towards the center of the sample (from 72 MPa to 82 MPa). Micro-mechanical tests were also confirmed by the observation of cross-linking changes (gel test) as well as crystallinity increases (wide-angle X-ray diffraction and microtome cuts). This finding could have a significant effect on the manufacturing and subsequent modification of injection-molded polypropylene parts, which opens new possibilities in practice for this material. The increased surface wear resistance enables the use of parts for which the durability and abrasion resistance of the surface are demanded, especially in applications facing exposure to long-term cyclical loads (e.g., gears).



Citation: Ovsik, M.; Stanek, M.; Dockal, A. Tribological and Micro-Mechanical Properties of Injected Polypropylene Modified by Electron Radiation. *Lubricants* **2023**, *11*, 296. <https://doi.org/10.3390/lubricants11070296>

Received: 15 June 2023

Revised: 3 July 2023

Accepted: 13 July 2023

Published: 15 July 2023



Copyright: © 2023 by the authors. Licensee MDPI, Basel, Switzerland. This article is an open access article distributed under the terms and conditions of the Creative Commons Attribution (CC BY) license (<https://creativecommons.org/licenses/by/4.0/>).

1. Introduction

Radiation modification of polymer properties is an ever-expanding field of work that generates progressively more interest from the industry. Use of this method requires a full understanding of radiation effects on polymer materials, especially when the goal is to improve their properties to higher levels [1–3].

Once the electron beam interacts with polymer material, its energy is absorbed by the polymer and an active particle (radical) is produced, due to which numerous chemical reactions commence. The following processes belong among these reactions:

- Cross-linking, which is when polymer chains link together in to a network;
- Chain scission, which leads to lower molecular weight of polymer;
- Oxidation, when polymer molecules react with oxygen (oxidation and chain scission often times appear concurrently);
- Chain branching, which is when polymer chains link, but 3D network is not yet created;
- Grafting, which is when a new monomer polymerizes and gets grafted on base polymer chain [1–8].

Varying polymers react differently to radiation, especially when it comes to cross-linking vs. chain scission. Parameter G is a widely used value defined as chemical gain depending on the number of reacting molecules per 100 eV of absorbed energy. Parameter

$G(X)$ describes how many transverse bonds are created in polymers per 100 eV of absorbed energy, while parameter $G(S)$ describes how many chains undergo scission per 100 eV of absorbed energy. Materials, where $G(S)/G(X) < 1$ apply are suitable for cross-linking. Materials with $G(S)/G(X) > 1$ are usually susceptible to degradation. Materials that possess both low $G(S)$ and $G(X)$ tend to be more resistant to radiation [1,2,4,6–8].

Cross-linking and chain scission are two competing processes that coexist during irradiation. The overall outcome of radiation depends on which of these has the upper hand at the observed time. Whenever the parameter $G(X)$ is greater than $G(S)$, the outcome is cross-linking. In the opposite case, the outcome is chain scission, i.e., degradation. The values of both parameters for any given polymer closely correspond with irradiation processing conditions, e.g., absorbed dose and temperature of irradiation. Both parameters increase with rising radiation doses. However, parameter $G(S)$ generally grows faster than $G(X)$. For this reason, three scenarios can occur concerning the relationship between polymer molecular weight (MW) and radiation dose (Figure 1) [1–8].

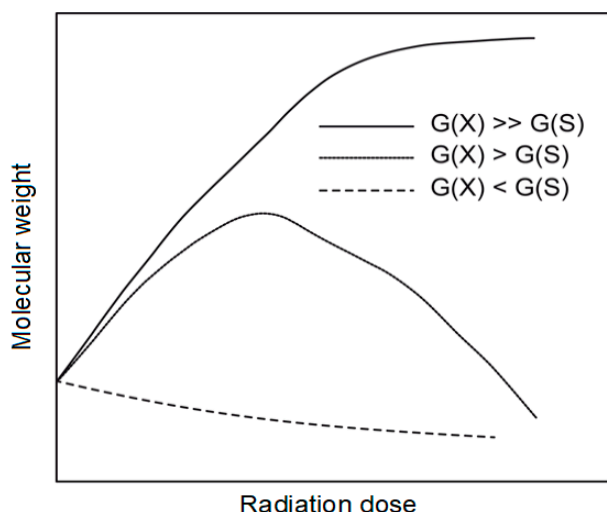


Figure 1. Relationship between polymer molecular weight (MW) and radiation dose.

In the first case, when $G(X)$ is much higher than $G(S)$, MW continually rises due to cross-linking, up until it plateaus due to $G(S)$ increasing faster. In the second case, when the $G(X)$ value is still higher but the difference is not so significant, the $G(S)$ value catches up, and a break on the MW curve that signifies a switch-over to degradation can be observed. Finally, when $G(S) > G(X)$, the material continually experiences degradation [1,2,4–8].

A study by Sirin et al. investigated the influence of radiation on polypropylene and polyethylene blend samples with varying weight ratios. Radiation doses of 10, 30, 50, 70, and 100 kGy were applied by a 60 Co source from polymer blends obtained from mixing polypropylene (PP) and polyethylene (LDPE). It was found that the melt temperatures of the blends were close to those of virgin polymers and that increasing the radiation dose slightly changed them. Overall, it can be said that the results of these polymer blends were important due to the improvement of some physical and thermal properties of polymers [9].

In another study, Yang et al. examined the effects of copper on a gamma-irradiated PP blend containing a cross-linking agent. The main finding of this research was the significant support that copper provides to the creation of a 3D network within PP blends during gamma radiation exposure. Copper in a PP structure accelerated the creation of free radicals in PP, which supports the creation of a cross-linked structure. The results of the gel test (60.65%), Melt Flow Index (MFI) test, and rheological analysis showed that the cross-linked structure hastened by the presence of copper was more pronounced with lower radiation levels (20 kGy) [10].

As stated in this article, gamma radiation has a significant influence on the modification and improvement of polymer materials. After radiation exposure, polymers were more

resistant to chemical reactions since there were no ingredients left to react with. Thus, polymers treated this way can be used in a wider temperature range for highly demanding applications, such as automotive, foil packaging, electric isolation, tissue engineering, medical device sterilization, biomedical and nuclear applications, and more [11–17].

Studies conducted by MS. Rahman et al. [18], Yang Di et al. [19], Baixing Liua et al. [20], and Natalia Wierzbická et al. [21] investigate the influence of electron radiation on the tribological properties of modified polymers. The results show that electron radiation has a positive influence on the tribological properties of varying types of polymers. Furthermore, higher radiation doses led to a decrease in tribological properties, which was caused by degradation processes.

Radiation cross-linking by beta electron radiation has found its place in various industrial fields, especially due to its advantages as a clean and safe technology. As a result of the immediate and precise delivery of the necessary radiation dosage, this technology has found its place in a diverse field of applications, e.g., isolation of cables and wires, heat-shrinkable foils and tubes, water pipes, and floor heating [22–28].

The aforementioned literary research is concerned with the description of the electron radiation effect on polymer properties. The presented studies describe parts of this as problematic, especially the influence of electron radiation on mechanical or tribological properties or the structure of polymers. There is no single study that deals with the influence of electron radiation on the micro-mechanical, tribological, and structural properties of polypropylene in a complex manner. The material polypropylene was chosen for this study, which is commonly used in technical practice for a number of structural applications and can also be easily modified using electron radiation. The current study deals with the influence of the penetration depth of an electron beam on the creation of structure, which results in varying micro-mechanical properties and tribological properties in individual layers of material.

2. Materials and Methods

Polypropylene, modified by electron radiation with an intensity range from 15 to 99 kGy, was chosen as the test material. Electron radiation causes cross-linking within the structure, but its effect is not uniform throughout its thickness. The change in properties was studied by micro-indentation tests with several loads (reaching differing depths) as well as across (cross-section) the material thickness. These changes were later confirmed by morphology measurements, such as the gel test and wide-angle X-ray diffraction. Each measurement was conducted at least 10 times and subsequently statistically evaluated by arithmetic mean and standard deviation.

2.1. Material

For the experiment, polypropylene (PP) with the trade name V-PTS-CREALEN-EP-2300L1*M800 (Dumfries, Scotland) was chosen as the test material. This polymer can be cross-linked by beta radiation only when enhanced with a special cross-linking agent. For this polypropylene, the cross-linking agent TAIC (Triallyl isocyanurate) in 6 vol. % was chosen. The entire TAIC-enhanced granulate preparation process was undertaken by PTS Plastic Technology Service.

2.2. Preparation of Test Samples

Test samples were manufactured by injection molding on ARBURG ALLROUNDER 470 E by Arburg (Losburg, Germany). Test samples were manufactured according to ČSN EN ISO 527-1 standard in a prism shape with the dimensions $4 \times 80 \times 10$ mm. Injection molding parameters were set according to the polymer manufacturer's recommendations, as can be seen in Table 1.

Table 1. Process parameters of injection molding (PP).

Technological Parameter	Unit	Value
Injection pressure	MPa	80
Injection speed	mm/s	50
Length of dose	mm	40
Temperature under hopper	°C	50
Cooling time	s	40
Holding pressure	MPa	8
Holding pressure duration	s	5
Heat zones settings		
Zone n. 1	°C	210
Zone n. 2	°C	220
Zone n. 3	°C	230
Zone n. 4	°C	240

Polypropylene was enriched by 6 vol. % of triallyl isocyanurate (TAIC), which is a cross-linking agent. During irradiation, TAIC enables free radicals in polypropylene to bond to the cross-linking agent and create a certain degree of cross-linking. The entire process of granulate preparation was carried out by PTS Plastic Technology Service.

The irradiation processes were conducted by BGS Beta-Gamma Service in Germany. The source of electron β -radiation was the high-voltage accelerator Rhodotron with a maximum energy of 10 MeV. Set doses of radiation were 15 kGy, 33 kGy, 45 kGy, 66 kGy, and 99 kGy.

2.3. Tribological Properties—Scratch Test

Tribological properties were measured using the MicroCombi tester MCT³ made by Anton Paar (Graz, Austria). The measurements were carried out by micro-indentation tests that enable the determination of the friction coefficient and resistance to abrasion of the studied surfaces. The principle of this measurement is based on a straight-forward motion of the indentor (Rockwell cone) with a 120° tip angle and a 100 μ m tip radius along the test sample surface. Measurements were carried out with constant loads (1 N and 5 N) and other process parameters, which can be seen in Table 2.

Table 2. Measurement parameters for tribological properties.

Measurement Parameter	Measurement 1	Measurement 2
Applied load (N)	1	5
Speed (mm/min)	10	10
Length (mm)	5	5
Acquisition Rate (Hz)	30	30

Ahead of the process, the indentor moves along the surface with a defined force to initiate the measurement device. Following the initiation, the indentor penetrates the test sample with normal force F_n , which leads to material deformation and the creation of an imprint. Sensors record the friction force F_t , which is proportional to normal force, in a so-called pre-scan that is concerned with the surface profile of the test sample before the penetration P_d (penetration depth) and post-scan of the imprint R_d (residual depth), which is important for polymer relaxation evaluation. The difference in profile depths ($P_d - R_d$) can be used to gain valuable information about the viscoelastic properties of material. Critical loads can be calculated precisely through acoustic emissions AE and friction coefficient μ .

2.4. Micro-Mechanical Properties

Micro-mechanical properties were measured by the instrumented hardness test with the DSI (depth sensing indentation) method on a MicroCombi tester MCT³ manufactured

by Anton Paar (Graz, Austria). The evaluation of measured mechanical properties was carried out according to ČSN EN ISO 14577-1. The set measurement parameters can be seen in Table 3. A Vickers four-sided pyramid with a tip angle of 136° was used as the indenter.

Table 3. Measurement parameters for micro-mechanical properties.

Measurement Parameters			
Applied load (N)	0.5	1	5
Load hold duration (s)	90	90	90
Loading/de-loading speed (m/s)	1	2	10
Poisson number	0.3	0.3	0.3

According to the aforementioned standard, the following parameters were evaluated: indentation hardness, indentation modulus, and indentation creep. The calculation of individual values was carried out using the method by Oliver and Pharr (Figure 2).

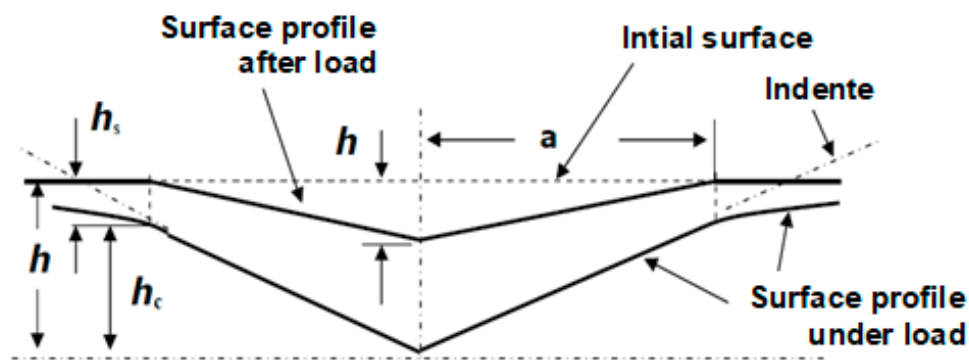


Figure 2. Schematic representation of the indentation processes showing the decreasing of the indentation depth during loading (according to Oliver and Pharr).

Indentation hardness H_{IT} represents the degree of resistance to permanent deformation or damage. Indentation hardness H_{IT} is generally defined as the maximum loading force P_{max} divided by the area of contact (A_p) between the indenter and test sample [29,30].

$$H_{IT} = \frac{F_{max}}{A_p} \quad (1)$$

$$A_p = 23.96 \times h_c^2 \quad (2)$$

Further material properties that can be gained from the indentation test conducted by the DSI method are the indentation modulus E_{IT} , reduced modulus E_r , and complex modulus E^* . In an ideal scenario, the indentation modulus has the exact same meaning as the elastic (Young) modulus. In general, the indentation modulus can be determined from the slope of the tangent line used for the calculation of the indentation hardness H_{IT} . The calculations involve the Poisson number (v_s), which is usually between 0.2 and 0.4 for metal materials and 0.3 and 0.4 for polymer materials [29,30].

$$E_{IT} = E^* \times (1 - v_s^2) \quad (3)$$

$$E^* = \frac{1}{\frac{1}{E_r} - \frac{1-v_i^2}{E_i}} \quad (4)$$

$$E_r = \frac{\sqrt{\pi}}{2 \times C \sqrt{A_p}} \quad (5)$$

If the change in the imprint's depth is measured during constant load, the relative depth of the indentation can be calculated; this value is called material creep. Equation (6) contains h_1 , which is the indentation depth in t_1 , the time when the maximum load is reached. Furthermore, h_2 is the depth reached in t_2 during the hold on constant maximum testing load phase [29,30].

$$C_{IT} = \frac{h_2 - h_1}{h_1} 100 \quad (6)$$

Micro-mechanical properties were measured on the surface layer (loads 0.5 N, 1 N, and 5 N) and individual depths under the surface (through cross-section) with a load of 0.5 N. For individual measurements at individual depths of the sample, the irradiated samples were cut into segments, fixed in resin, and polished.

Samples were cut using a laboratory linear saw, IsoMet 4000, manufactured by Buehler (Leifelden-Echterdingen, DE), which utilizes a diamond grinding wheel. During cutting, the sample was cooled by liquid brought to the cutting space of the wheel. The revolutions of the saw were set to 1800 rpm.

Individual segments were fixed into resin on a SimpliMet 1000 press provided by Buehler. An Automatic press, SimpliMet 1000, is generally used to produce thermoplastic and thermoset test samples. The following parameters were set: heating time (1:30 min), cooling time (4 min), pressing pressure (290 bars), sample diameter (40 mm), and pressing temperature (150 °C). PhenoCure resin, made by Buehler, was used as powder for the sample fixture.

The samples in resin were first ground by EcoMet 250 with a rotating head AutoMet 250, both also manufactured by Buehler. The process started with the following parameters: head rotation revolution (40 rpm), table revolution (100 rpm), and pressing force (20 N), which made the samples adhere to the grinding wheel. Water was delivered to the grinding plane in order to improve the cooling effect and carry away chipping residue. The grinding was carried out in multiple steps with grinding wheels of varying textures (P180, P320, P600, and P1200). Then, the samples were polished in diamond suspension with 9 and 3 μm particles. Polishing was conducted without additional cooling.

2.5. Morphology

The results of the instrumented hardness tests and polymer morphology changes induced by cross-linking were evaluated by the gel test and wide-angle X-ray diffraction.

2.5.1. Gel Test

The degree of cross-linking was determined by the gel test, which was carried out according to the EN ISO 579 standard. The general procedure of the gel test starts with the preparation of 1 g of irradiated material, with precision to three decimal places, which is then mixed with 100–250 mL of solvent. Test samples in this work were made out of PP, which has an amorphous part that can be dissolved by Xylol while the cross-linked part remains intact.

The mixture is left to extract for 6 h. Afterwards, distillation is used to separate the soluble parts. In order to remove the remaining Xylol, the cross-linked extract is washed in distilled water. The extract is purified this way and then dried for 6–8 h with lowered pressure in a vacuum drier at 100 °C. After it is completely dried and cooled, the remaining sample can then be weighted again to three decimal places and compared with its original weight. The result is given in percent as a degree of cross-linking.

2.5.2. Wide-Angle X-ray Diffraction

This method was used to determine the crystalline structure of both the surface layer and the center layer. WAXD was carried out on a X'PERT PRO MPD (MultiPurpose Diffractometer) with a monochromatic radiation CuK α and nickel filter. The device was manufactured by PANalytical (Malvern, UK). All measurements were conducted at 40 kV and 30 mA, while the angle of the rays was between 10° and 30° with 0.013° steps.

2.5.3. Optical Microscopy—Microtome Cuts

When the samples were prepared, the slices were cut transversely to a 40 μm thickness on a rotational microtome Leica RM 2255 (Deer Park, IL, USA). These cuts were examined using a polarized optical microscope, which enabled observation of the structure along the entire cross-section.

2.5.4. Transmission Electron Microscope

Electron microscopy was performed on a transmission electron microscope, Tesla 500 (Prague, Czech Republic), at 90 kV using replicas of selectively etched sample surfaces. Selective etching was performed using a 1% solution of KMnO₄ in 85% H₃PO₄ for 1 to 10 min at room temperature. After selective etching, the samples were vacuum-shadowed by gold or platinum. For sample replication, a 5% water solution of polyacrylic acid was used. The magnification of the micrographs is indicated by 1 mm bars and the extension direction by an arrow.

3. Results

The results reflect the influence of electron radiation and the depth of penetration on morphology, which were measured by the gel test and wide-angle X-ray diffraction. This treatment affected the final tribological and mechanical properties (indentation hardness, indentation modulus, and indentation creep) and did so differently throughout the individual layers.

3.1. Tribological Properties

Tribological properties, e.g., friction force (Figures 3a and 4a), acoustic emission (Figures 3b and 4b), friction coefficient (Figures 3c and 4c), and surface profile after indentation (Figures 3d and 4d) of the modified polypropylene surface, can also be investigated using the scratch test. These tests can help with the prediction of surface resistance to abrasion. Tribological properties were measured in samples irradiated by selected doses of radiation (0, 33, 66 and 99 kGy) for improved clarity of results.

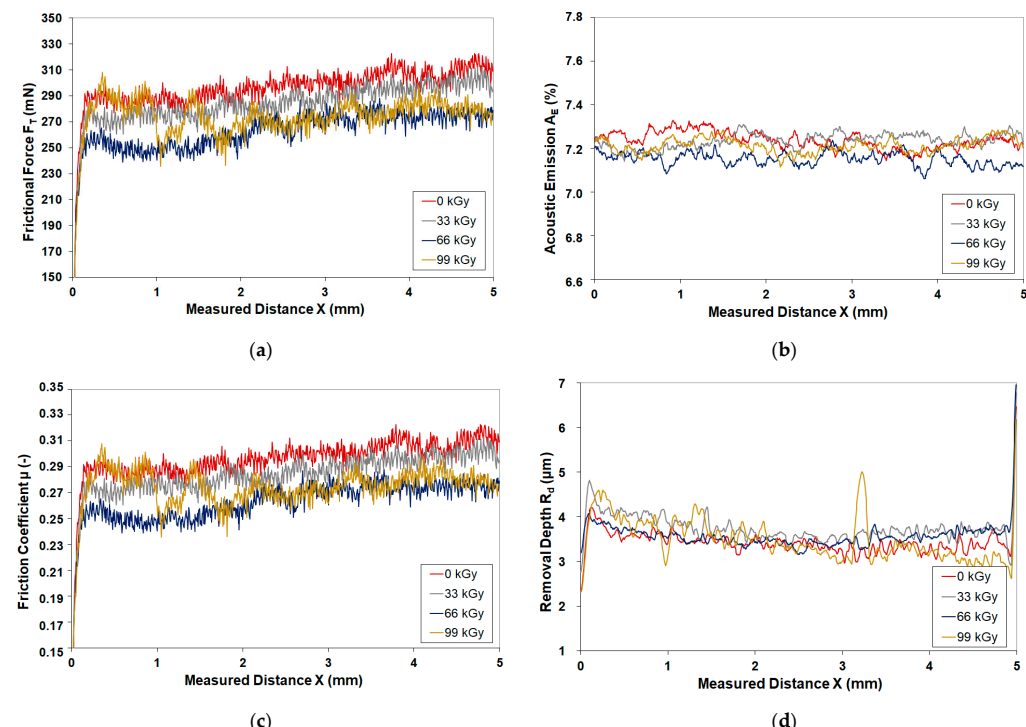


Figure 3. Tribological properties 1 N: (a) Frictional force; (b) Acoustic emission; (c) Friction coefficient; (d) Removal depth.

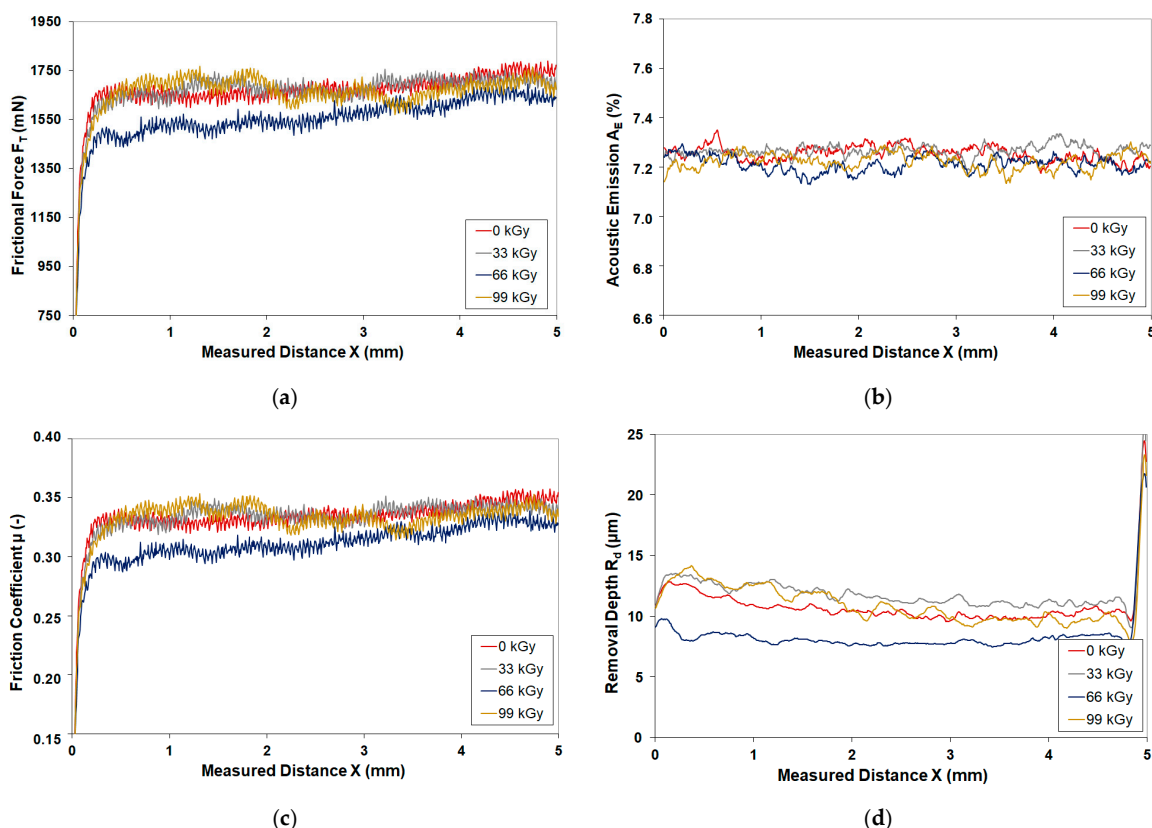


Figure 4. Tribological properties 5 N: (a) Frictional force; (b) Acoustic emission; (c) Friction coefficient; (d) Removal depth.

The results of tribological tests carried out with a loading force of 1 N show that the highest values of observed properties, e.g., friction force, acoustic emission, and friction coefficient, were found in virgin PP. On the contrary, the observed tribological properties improved in radiation modified PP. The lowest tribological properties were found in specimens irradiated with 66 kGy. For example, the friction coefficient was 0.31 for virgin PP, but only 0.27 for PP exposed to 66 kGy.

Tribological properties measured with a loading force of 5 N displayed similar tendencies to those measured with 1 N. The highest values were found in virgin PP, while the lowest values were observed in PP irradiated by 66 kGy. For example, the friction coefficient was 0.36 for the former and 0.32 for the latter.

Radiation modification improved the tribological properties, which led to an increase in resistance to surface wear. This enhancement was caused by structural changes that directly impacted the micro-mechanical properties. These changes guarantee that the product can be used in demanding conditions that require high surface resilience.

3.2. Micro-Mechanical Properties

The DSI method is used not only for the measurement of polypropylene hardness/micro-hardness but also for recording indentation characteristics throughout the process. This method records continuous changes in indentation depth depending on time. Figure 1 shows the selected indentation curves, i.e., the course of indentation force in dependence on the increasing indentation depth (Figure 5a) and the course of indentation depth in time (Figure 5b), for virgin PP and one irradiated by 45 kGy under three different loads (0.5 N, 1 N, 5 N). The highest micro-mechanical properties were measured in PP irradiated by 45 kGy. Individual dependencies can be used to determine material behavior as well as the depth of indentation reached for individual loads.

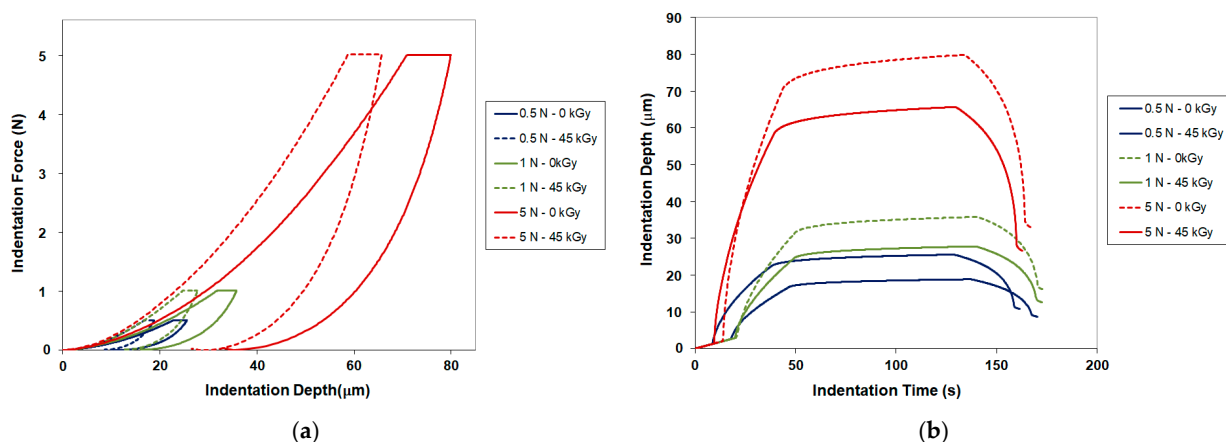


Figure 5. Indentation curves for loads 0.5 N, 1 N and 5 N (0 and 45 kGy): (a) indentation force dependence on indentation depth; (b) Indentation depth dependence on indentation time (creep).

Figure 5a shows the dependence of loading force on indentation depth. As can be seen, the highest indentation (60 μm) for PP irradiated by 45 kGy was observed in PP irradiated by 45 kGy measured with a 5 N loading force. At 1 N, the indentation was approximately 30 μm , while the lowest depth (20 μm) was reached under 0.5 N. Indentation dependence is characterized by loading area (the indentor steadily climbs to the maximum load), holding area, and de-loading area (the indentor gradually decreases the load all the way to zero). Based on these courses and the detection of the immediate position of the indentor in dependence on loading force, it is possible to evaluate the mechanical properties, such as indentation hardness and modulus, of the tested PP.

Figure 5b characterizes the dependence of indentation depth on time with the application of a constant loading force. The time course of indentation depth is quite important for the determination of polymer creep behavior. Indentation creep can be calculated from the holding phase, when the indentor changes depth even with a constant load (indentor sinking), which leads to material creep.

The primary value gained from the instrumented hardness test is indentation hardness. Indentation hardness is characterized by its degree of resistance to permanent deformation or damage and is defined as the maximum loading force divided by the contact area.

The graphical evaluation of the measured indentation hardness results of dependence on varying doses of radiation and differing loading forces for PP can be seen in Figure 6a. The values of indentation hardness for PP are significantly influenced by the magnitude of the loading force. The values of indentation hardness rose notably with an increase in loading force. The measured values indicate that radiation cross-linking manifests in the improved hardness of the tested polymer. The lowest value for all test samples was measured in virgin polymer (38 MPa), while the highest hardness value was measured in PP irradiated by 45 kGy. Doses higher than 45 kGy led to a decrease in indentation hardness. The maximum indentation hardness (56 MPa) for loading forces of 0.5 N was measured in samples irradiated with 45 kGy. The difference in hardness between virgin PP and PP exposed to radiation was 47%. The maximum indentation hardness for loading force 1 N was measured in the same sample, but this time it was 67 MPa, thus the difference in hardness in comparison with virgin polymer rose to 76%. Finally, the same sample was responsible for the highest indentation hardness (78 MPa), which was a 105% difference compared to the unaltered polymer. Higher doses of radiation led to a significant decrease in indentation hardness, which was basically 12% for all loads. The decrease in hardness values after the application of radiation doses higher than 45 kGy was caused by material degradation, which was subsequently confirmed by gel tests and wide-angle X-ray diffraction.

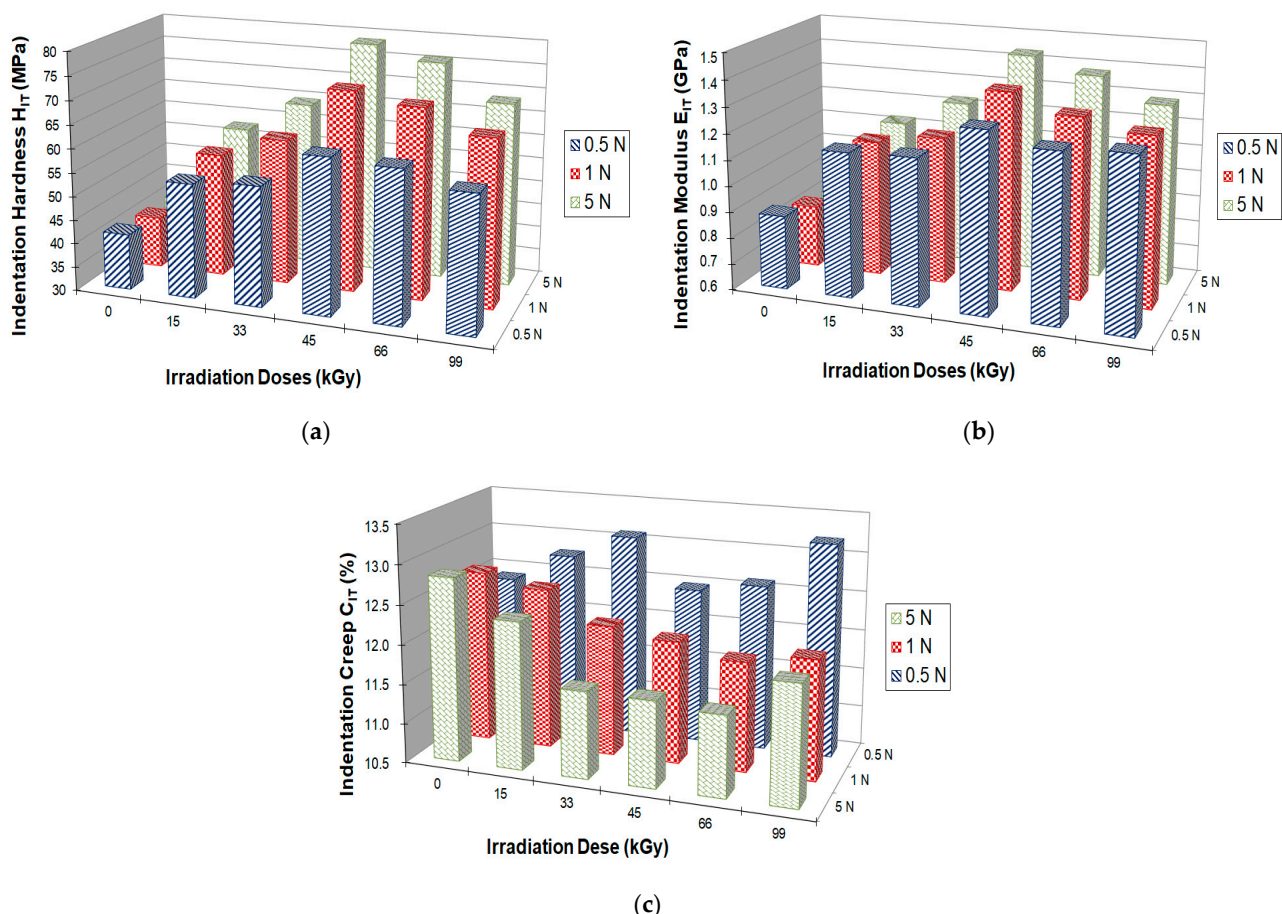


Figure 6. Dependence of mechanical properties on radiation dose for loading forces 0.5 N, 1 N and 5 N: (a) Indentation hardness; (b) Indentation modulus; (c) Indentation creep.

Another important value that can be gained from the instrumented hardness test is the indentation modulus. This modulus can be determined from the slope of the de-loading curve and corresponds with the elastic (Young) modulus.

Regarding indentation hardness (Figure 6a), similar results were also measured for indentation modulus (Figure 6b), which closely corresponds with indentation hardness. The highest values of indentation modulus for all loading forces (0.5 N, 1 N and 5 N) were found in PP irradiated by 45 kGy. For loading forces of 0.5 N, the difference between virgin and irradiated PP was 45%, while for 1 N, it was 62%. The biggest difference was found in samples with a loading force of 5 N, which was 77%. As can be seen from measurements performed at varying loading forces, increasing force (depth of measurement) led to a higher indentation modulus. This finding corresponds with crystallinity measurements, which indicated higher crystallinity with higher depth. On the other hand, the lowest values of the indentation modulus were found in virgin PP, as is evident from Figure 6b. Higher doses of radiation led to a decrease in indentation modulus, which could be caused by material degradation due to the high intensity of radiation. Measurements of indentation modulus correspond with material tendencies that were also found during tensile tests and elastic modulus measurements.

The instrumented hardness test was used to study the influence of radiation dose on the creep behavior of the tested PP. The characteristic value, the indentation creep, can be determined from the dependence of indentation depth on indentation time. Indentation creep manifests by itself in the gradual sinking of the indentor.

The course of indentation depth change in dependence on time while the sample was experiencing a constant loading force can be seen in Figure 6c. The measurements show that radiation cross-linking positively affects the creep behavior (indentation creep) of the

studied PP. Measurements gained by the instrumented hardness test showed the lowest values of indentation creep in PP irradiated by 45 kGy, where it was 15% lower when compared with virgin polymer. The highest value of indentation creep was measured in PP irradiated by 99 kGy. Higher values led to a significant increase in indentation creep, which could be caused by the degradation of the studied polymer, especially in the surface layer. It is evident from a comparison of indentation creep results with hardness that a correlation can be found, i.e., increasing hardness led to a decrease in indentation creep.

3.3. Micro-Mechanical Properties—Section across Sample

Indentor dimensions and extraordinarily precise positioning enables the use of the DSI method in studies of indentation hardness and numerous other characteristics describing micro-mechanical behavior through cross-sections of tested samples. A schematic description of the test through the cross-section can be seen in Figure 7. The tested sample was cut in the center, and its mechanical properties were measured from one edge to the opposite one (0 mm, 0.6 mm, 1.3 mm, 2 mm, 2.7 mm, 3.4 mm, and 4 mm).

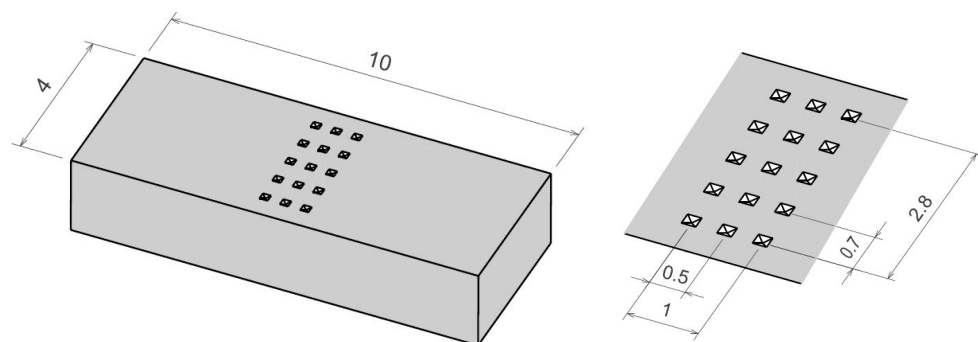


Figure 7. Schematic description of measurement through test sample's cross-section.

As is obvious from Figure 8a, the DSI method was used to measure indentation hardness across the entire thickness of both the virgin samples and PP irradiated by varying doses of beta radiation. The indentation hardness increased with increasing distance from the surface for all doses of radiation. Specifically, indentation hardness measured in PP irradiated by 45 kGy was 14% higher 2 mm from the edge than it was at the surface layer. On the contrary, indentation hardness for virgin PP was approximately the same across the entire thickness. These results correspond with mechanical property measurements for varying loads, in which the highest depth, thus hardness, was reached with a loading force of 5 N. These changes were caused by varying crystallinity in individual layers, as shown by wide-angle X-ray diffraction.

Similar tendencies across the sample thickness were measured for indentation modulus as for indentation hardness. The indentation modulus once again increased with increasing distance from the surface, and it was 28% larger 2 mm from the edge than at the edge itself. As can be seen in Figure 8b, the values for unaltered PP were evenly distributed across the thickness of the test sample.

The results of indentation creep (Figure 8c) point towards an improvement trend from the edge to the center of the sample. The difference between the surface and center of the sample was approximately 30%. These tendencies emerged in all samples, which were irradiated with varying doses of radiation.

The results of indentation properties gained by the DSI method through the cross-section of test samples correspond with structural measurements carried out by wide-angle X-ray diffraction. Lower mechanical property values were measured at the surface layer of tested PP than at the center, which coincides with the changing crystalline and amorphous content.

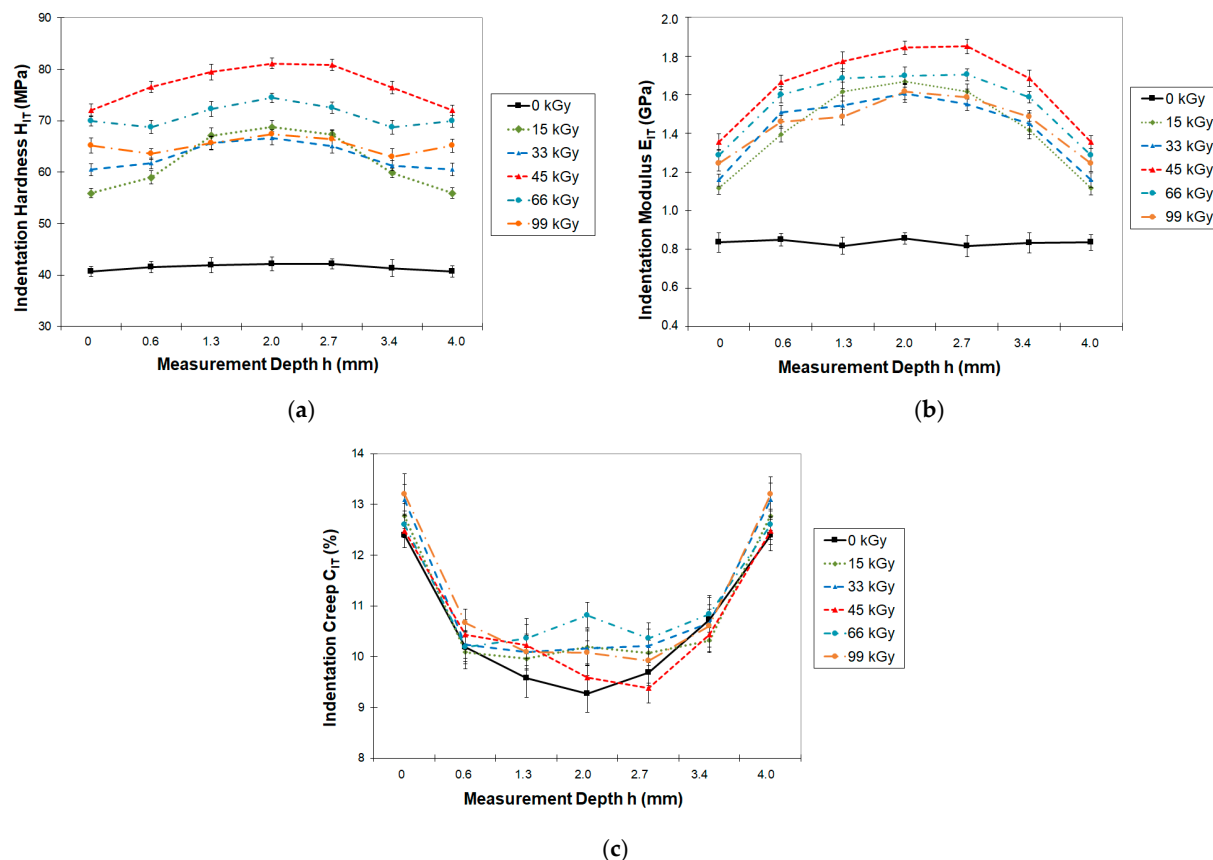


Figure 8. Mechanical properties through test sample's cross-section (0–99 kGy): (a) Indentation hardness; (b) Indentation modulus; (c) Indentation creep.

3.4. Morphology—Change of Structure

Morphology (structure) measurements were conducted in order to confirm the results and changes in PP micro-mechanical properties measured by DSI. The goal of these measurements was to interpret changes in the structure and morphology of PP irradiated by beta radiation.

3.4.1. Degree of Cross-Linking

In general, a gel test is conducted to measure the degree of cross-linking (content of gel) in the tested polymer. The degree of cross-linking in PP in dependence on the applied radiation dose is evident in Figure 9. The maximum gel content was found in PP exposed to 45 kGy of radiation. As is obvious from Figure 8, the degree of cross-linking (gel content) is directly responsible for the properties of the irradiated polymer. Higher doses pointed towards a slight decrease in cross-linking and thus in mechanical property values. This could be caused by material degradation due to high radiation intensity.

3.4.2. Wide-Angle X-ray Diffraction

Wide-angle X-ray diffraction was used to measure the change in crystalline and amorphous phase content, conducted both on the surface (Figure 10a) and at the center (Figure 10b) of the tested polymer sample. As is evident from the results, neither the position nor intensity of the peaks changed with the increasing growth of radiation. The width of the peaks represents the size of the crystals, and it changes only slightly. A comparison of the position and size of the peaks between the surface and center of the part shows that there were slight differences that manifested as variations in crystallinity. The crystallinity content was determined by measuring the surface area of the amorphous and crystalline parts of the studied polypropylene. As can be seen in Figure 11, increasing

the dose of radiation led to significant changes in crystalline phase content. The application of electron radiation led to changes in the polypropylene structure and its crystalline phase. Radiation-induced cross-linking was observed in the amorphous phase, which has a significant effect on the micro-mechanical properties of the surface layer. The measured results of WAXD imply that the lowest crystalline phase content was present in virgin PP and PP irradiated by 15 kGy, 66 kGy, and 99 kGy, which at the same time demonstrated the lowest values of micro-hardness and micro-toughness in the surface layer. With radiation doses of 33 kGy and 45 kGy, there is a significant increase in crystalline phase content, which once again corresponds with the improved values of micro-hardness and micro-toughness. The increase in crystalline phase content results in a more prominent improvement in micro-hardness in comparison with changes in amorphous content. As can be seen from Figure 11, a higher crystalline phase content was found in the middle of the tested sample than at the surface. High doses of radiation correlate with structure changes, i.e., radiation melting. Radiation melting involves pushing defects or irregularities in crystalline lamella to the surface. It is most likely caused by the transport of energy by excitons along macromolecules, which leads to more defects in the surface of the lamella, which correspondingly becomes thinner. Cross-linking and degradation processes happen at the same time, especially in disorganized zones.

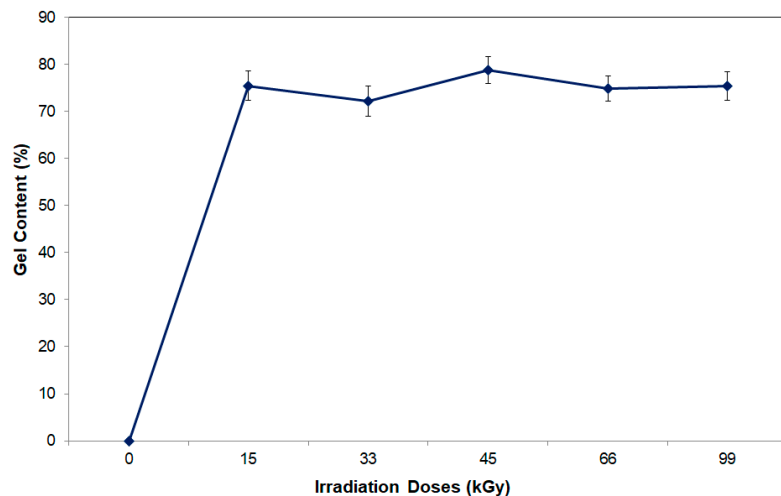


Figure 9. Degree of cross-linking in dependence on radiation dose.

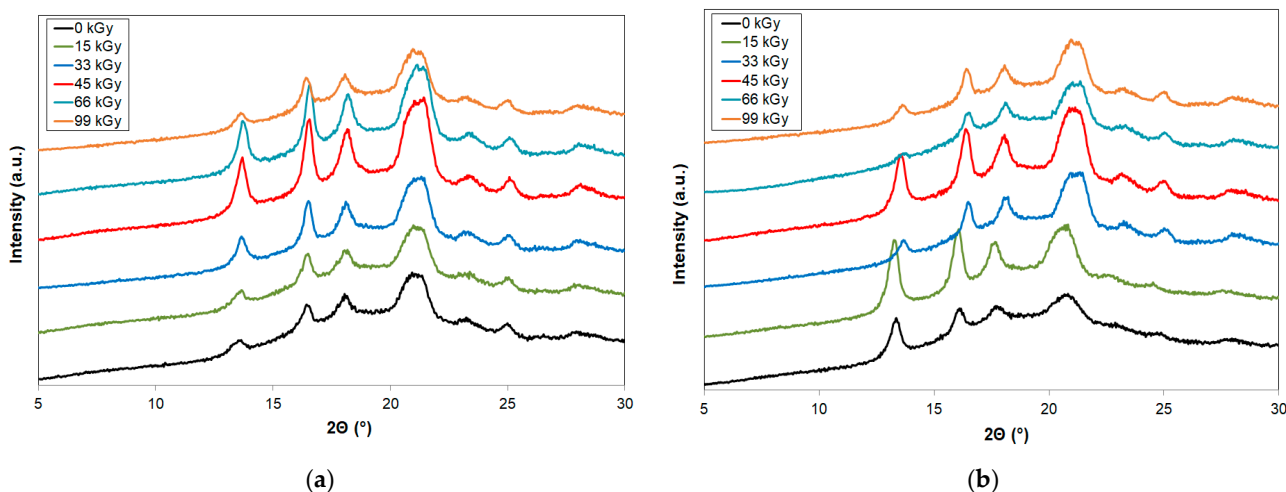


Figure 10. Wide-angle X-ray diffraction: (a) surface of sample; (b) center of sample.

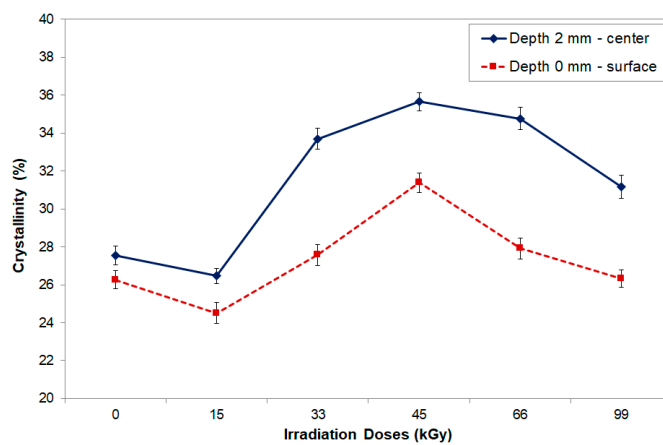


Figure 11. Change of crystallinity in dependence on depth of measurement.

The DSI method can record and quantify changes in the mechanical behavior of individual layers of the tested polymer sample.

3.4.3. Microscope Images of Microtome Cuts

After the samples were cut and their micro-mechanical properties were measured by the DSI method, microtome cuts were prepared for each sample with varying exposure to radiation doses. As can be seen in Figure 12, the increase in radiation dose led to changes in crystalline phase content. As can be seen from associated microtome cuts, increasing the dose of radiation led to changes in skin-core structure. Higher doses of radiation led to thinning of the skin layer and varying sizes and volumes of the crystalline phase in the core layer. The skin layer was 100 µm in virgin PP, while it was only 20 µm in samples irradiated by 45 kGy and almost non-existent in samples exposed to 99 kGy. This also impacted changes in micro-mechanical and tribological properties. These results were also confirmed by wide-angle X-ray diffraction and Transmission electron microscopy.

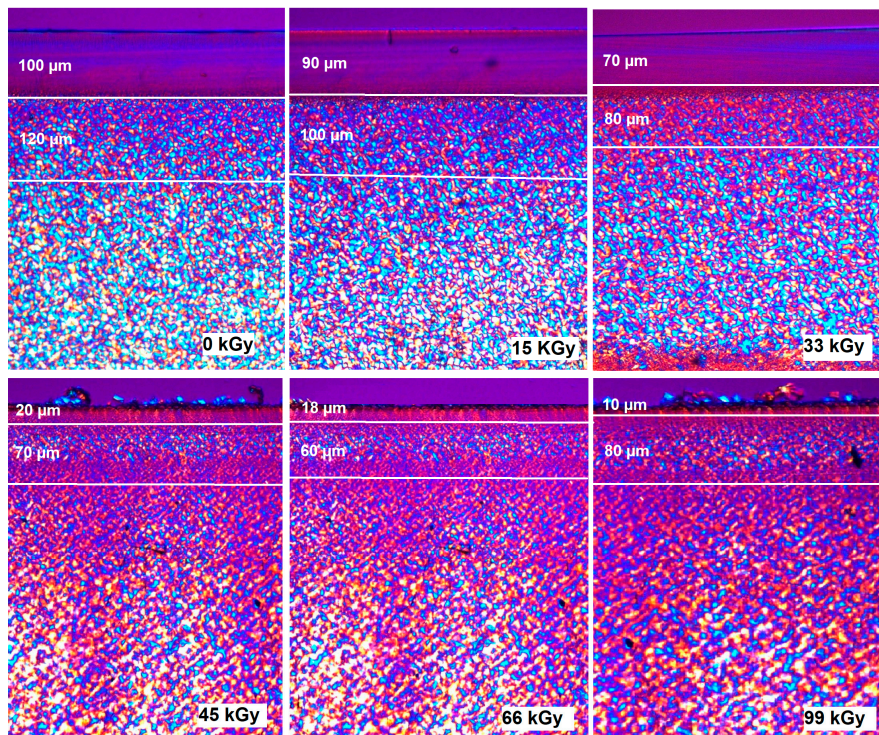


Figure 12. Microtome cuts images.

3.4.4. Transmission Electron Microscopy

The morphology of irradiated and virgin polypropylene was also observed by transmission electron microscopy. The final structure contained mostly spherulites. Observed structures were most prominent in samples irradiated by 45 kGy. The use of higher doses (90 kGy) led to the partial degradation of polypropylene (Figure 13), which indicates a decrease in micro-mechanical properties in surface layers. These results confirm the findings of previous morphology tests.

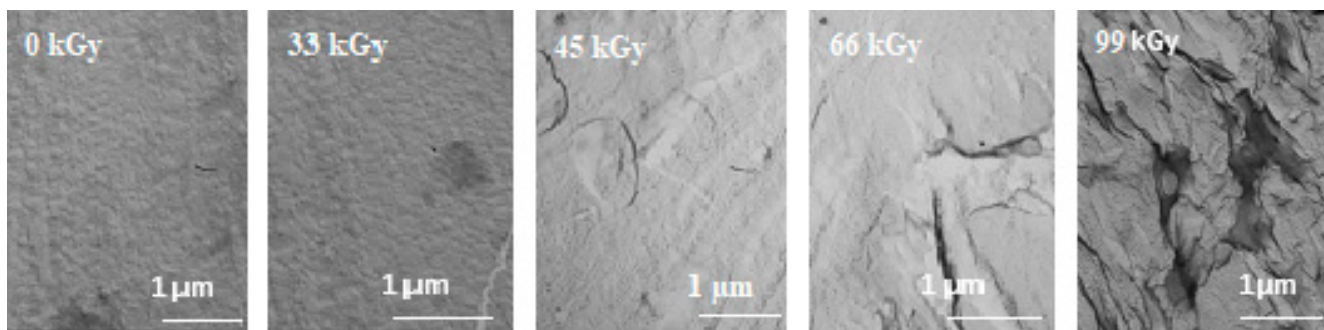


Figure 13. Transmission electron microscope of the irradiated polypropylene.

The results gained from the instrumented hardness test were supported by structure measurements, i.e., gel tests, wide-angle X-ray diffraction, polarized optical microscope images of microtome cuts, and Transmission electron microscopy. As is evident from the results, there was a change in crystalline and amorphous content in both the surface layer and layers within the sample, which corresponds with changes in micro-mechanical and tribological properties.

As shown by previous measurements, the best values of micro-mechanical and tribological properties were found in test samples irradiated by 45 kGy, which was caused by the creation of a 3D network (measured by gel test) and increased crystalline phase content. Higher doses of radiation led to degradation processes, which were supported by the results of the gel test and decreased crystalline phase. Degradation processes led to a decline in observed properties. These results confirm the findings of various authors [1–29] who have investigated this topic in publications presented in the literature.

The results of this study investigate the dependence of the surface wear of PP on its resilience. The polypropylene was modified by electron radiation, which manifested in improved tribological properties of the surface layer and micro-mechanical properties through the material cross-section. These properties demonstrate the usability of this modification when enhanced surface resilience is needed and enable the use of cheaper materials in place of expensive ones. This improvement was caused by structure changes induced by electron radiation that influenced crystallinity, the degree of cross-linking, and skin-core layers.

4. Conclusions

Radiation cross-linking has a positive influence on tribological and micro-mechanical properties measured by instrumented hardness tests, especially friction coefficient, indentation hardness, modulus, and creep. The optimal radiation exposure for the tested material with the given composition appears to be 45 kGy (66 kGy), which was the threshold where tribological and micro-mechanical properties were at their peak. The measurements show that these micro-mechanical properties were not homogenous across the thickness of the samples. Towards the center of the tested PP, an increasing trend was found in mechanical properties. The difference between the surface and center of the tested PP was up to 28%. This finding was confirmed by morphology measurements carried out by wide-angle X-ray diffraction that showed changes in crystallinity phase content in both the surface layer and center layer. The results show that electron radiation has an influence on crystallinity,

which was 12% higher in the center layer than it was in the surface layer. Confirmation of cross-linking was carried out by gel tests, which showed the highest cross-linking for test samples irradiated by 45 kGy. Higher doses led to a decrease in mechanical properties, which could be caused by degradation processes due to high radiation intensity. So, concrete applications need a specific radiation intensity that is suitable. Due to increased tribological and micro-mechanical properties, increased resistance to wear was gained in irradiated materials. This modification of materials enables the use of cheaper polymers in applications with high requirements for long-term resistance against wear.

Author Contributions: Conceptualization, M.O.; methodology, M.O. and M.S.; formal analysis, M.S. and A.D.; data curation, M.O. and M.S.; writing—original draft preparation, M.O.; visualization, M.O.; project administration, M.O.; funding acquisition, M.S. All authors have read and agreed to the published version of the manuscript.

Funding: This article was written with the support of the project TBU in Zlin Internal Grant Agency: No. IGA/FT/2023/005.

Institutional Review Board Statement: Not applicable.

Informed Consent Statement: Not applicable.

Data Availability Statement: The data presented in this study are available on request from the corresponding author.

Conflicts of Interest: The authors declare no conflict of interest.

References

- Makuuchi, K.; Cheng, S. *Radiation Processing of Polymer Materials and Its Industrial Applications*; Wiley: Hoboken, NJ, USA, 2012; p. 415.
- Drobny, J.G. *Ionizing Radiation and Polymers: Principles, Technology and Applications*; Elsevier/William Andrew: Oxford, UK, 2013; p. 298.
- Gheysari, D.; Behjat, A.; Haji-Saeid, M. The effect of high-energy electron beam on mechanical and thermal properties of LDPE and HDPE. *Eur. Polym. J.* **2001**, *37*, 295–302. [[CrossRef](#)]
- Satapathy, S.; Chattopadhy, S.; Chakrabarty, K.K.; Nag, A.; Tiwari, K.N.; Tikku, V.K.; Nando, G.B. Studies on the effect of electron beam irradiation on waste polyethylene and its blends with virgin polyethylene. *J. Appl. Polym. Sci.* **2006**, *101*, 715–726. [[CrossRef](#)]
- Reichmanis, E.; Frank, F.; O'donnell, J.H. *Irradiation of Polymeric Materials: Processes, Mechanisms, and Applications*; American Chemical Society: Washington, DC, USA, 1993; p. 338.
- Clegg, D.; Collyer, A. *Irradiation Effects on Polymers*; Elsevier Applied Science: London, UK, 1991; p. 450.
- Gehring, J.; Zyball, A. Radiation crosslinking of polymers-status, current issues, trends and challenges. *Radiat. Phys. Chem.* **1995**, *46*, 931–936. [[CrossRef](#)]
- Clough, R.L.; Shalaby, W. *Irradiation of Polymers: Fundamentals and Technological Applications*; American Chemical Society: Washington, DC, USA, 1996; p. 433.
- Sirin, M.; Zeybek, M.S.; Sirin, K.; Abali, Y. Effect of gamma irradiation on the thermal and mechanical behaviour of polypropylene and polyethylene blends. *Radiat. Phys. Chem.* **2022**, *194*, 110034. [[CrossRef](#)]
- Yang, T.H.; Cheng, Y.C.; Wu, Y.P.; Yu, B.; Huang, T.; Yu, H.; Zhu, M.F. Enhanced crosslinking of polypropylene in gamma-irradiation via Copper (II) doping. *Radiat. Phys. Chem.* **2022**, *194*, 110042. [[CrossRef](#)]
- Naikwadi, A.T.; Sharma, B.K.; Bhatt, K.D.; Mahanwar, P.A. Gamma Radiation Processed Polymeric Materials for High Performance Applications: A Review. *Front. Chem.* **2022**, *10*, 837111. [[CrossRef](#)]
- Abraham, A.C.; Czayka, M.A.; Fisch, M.R. Electron beam irradiations of polypropylene syringe barrels and the resulting physical and chemical property changes. *Radiat. Phys. Chem.* **2010**, *79*, 83–92. [[CrossRef](#)]
- Ashfaq, A.; Clochard, M.C.; Coqueret, X.; Dispenza, C.; Driscoll, M.S.; Ułański, P.; Al-Sheikhly, M. Polymerization Reactions and Modifications of Polymers by Ionizing Radiation. *Polymers* **2020**, *12*, 2877. [[CrossRef](#)]
- Han, D.H.; Shin, S.H.; Petrov, S. Crosslinking and degradation of polypropylene by electron beam irradiation in the presence of trifunctional monomers. *Radiat. Phys. Chem.* **2004**, *69*, 239–244. [[CrossRef](#)]
- Wang, H.T.; Jiang, H.Q.; Shen, R.F.; Ding, X.J.; Zhang, C.; Li, L.F.; Li, J.Y. Electron-beam radiation effects on the structure and properties of polypropylene at low dose rates. *Nucl. Sci. Tech.* **2018**, *29*, 87. [[CrossRef](#)]
- Hu, J.; Zhao, X.C.; Xie, J.H.; Liu, Y.; Sun, S.L. Enhanced dielectric and energy storage properties of polypropylene by high-energy electron beam irradiation. *Polym. Eng. Sci.* **2022**, *62*, 1756–1763. [[CrossRef](#)]
- Okuhara, M.; Nomura, R.; Nishi, Y. Improvements of Elasticity and tensile strength of Glass Fiber Reinforced Thermoplastic Polypropylene by Electron Beam Irradiation. *J. Jpn. Inst. Met. Mater.* **2016**, *80*, 360–364. [[CrossRef](#)]

18. Rahman, M.S.; Shaislamov, U.; Yang, J.K.; Kim, J.K.; Yu, Y.H.; Choi, S.; Lee, H.J. Effects of electron beam irradiation on tribological and physico-chemical properties of Polyoxymethylene copolymer (POM-C). *Nucl. Instrum. Methods Phys. Res. Sect. B Beam Interact. Mater. At.* **2016**, *387*, 54–62. [[CrossRef](#)]
19. Yang, D.; Xie, G.; Cao, C. The effect of gamma irradiation on the tribological properties of UHMWPE composite filled with HDPE. *J. Thermoplast. Compos. Mater.* **2014**, *27*, 1045–1053.
20. Liu, B.; Pei, X.; Wang, Q.; Sun, X.; Wang, T. Effects of proton and electron irradiation on the structural and tribological properties of MoS₂/polyimide. *Appl. Surf. Sci.* **2011**, *258*, 1097–1102. [[CrossRef](#)]
21. Wierzbicka, N.; Sterzyński, T.; Nowicki, M. The Friction of Structurally Modified Isotactic Polypropylene. *Materials* **2021**, *14*, 7462. [[CrossRef](#)]
22. Manas, D.; Ovsik, M.; Mizera, A.; Manas, M.; Hylova, L.; Bednarik, M.; Stanek, M. The Effect of Irradiation on Mechanical and Thermal Properties of Selected Types of Polymers. *Polymers* **2018**, *10*, 158. [[CrossRef](#)] [[PubMed](#)]
23. Drobny, J.G. *Radiation Technology for Polymers*; CRC Press: Boca Raton, FL, USA, 2010.
24. Dadbin, S.; Frounchi, M.; Saeid, M.H.; Gangi, F. Molecular Structure and Physical Properties of EBeam Crosslinked Low-Density Polyethylene for Wire and Cable Insulation Applications. *J. Appl. Polym. Sci.* **2002**, *86*, 1959–1969. [[CrossRef](#)]
25. Toselli, M.; Saccani, A.; Pilati, F. Thermo-oxidative resistance of crosslinked polyethylene (XLPE) coated by hybrid coatings containing graphene oxide. *Surf. Coat. Technol.* **2014**, *258*, 503–508. [[CrossRef](#)]
26. Qureshi, M.I.; Malik, N.H.; Al-Arainy, A.A. Impact of cations toward the water tree propensity in crosslinked polyethylene insulation. *J. King Saud Univ.-Eng. Sci.* **2011**, *23*, 43–48. [[CrossRef](#)]
27. Kelley, K.M.; Stenson, A.C.; Dey, R.; Whelton, A.J. Release of drinking water contaminants and odor impacts caused by green building cross-linked polyethylene (PEX) plumbing systems. *Water Res.* **2014**, *67*, 19–32. [[CrossRef](#)] [[PubMed](#)]
28. Roumeli, E.; Markoulis, A.; Kyratsi, T.; Bikaris, D.; Chrissafis, K. Carbon nanotube-reinforced crosslinked polyethylene pipes for geothermal applications: From synthesis to decomposition using analytical pyrolysis—GC/MS and thermogravimetric analysis. *Polym. Degrad. Stab.* **2014**, *100*, 42–53. [[CrossRef](#)]
29. Oliver, W.C.; Pharr, G.M. Measurement of hardness and elastic modulus by instrumented indentation: Advances in understanding and refinements to methodology. *J. Mater. Res.* **2004**, *19*, 3–20. [[CrossRef](#)]
30. Ovsik, M.; Stanek, M.; Stanek, M.; Dockal, A.; Vanek, J.; Hylova, L. Influence of Cross-Linking Agent Concentration/Beta Radiation Surface Modification on the Micro-Mechanical Properties of Polyamide 6. *Materials* **2021**, *14*, 6407. [[CrossRef](#)] [[PubMed](#)]

Disclaimer/Publisher's Note: The statements, opinions and data contained in all publications are solely those of the individual author(s) and contributor(s) and not of MDPI and/or the editor(s). MDPI and/or the editor(s) disclaim responsibility for any injury to people or property resulting from any ideas, methods, instructions or products referred to in the content.